PLGA-based particulate vaccine delivery systems for immunotherapy of cancer

Monteiro Garrido Castro e Silva, Ana Luisa

Chapter 6

Co-encapsulation of synthetic long peptide antigen and Toll like receptor 2 ligand in poly-(lactic-co-glycolic-acid) particles results in sustained MHC class I cross-presentation by dendritic cells

Rodney A. Rosalia,*, Ana Luisa Silva*, Ivan Stepanek, Annelies van der Laan, Jaap Oostendorp, Wim Jiskoot, Sjoerd Van der Burg, Ferry Ossendorp

*contributed equally to this study

Manuscript in preparation for publication

Abstract

We previously reported the succesfull incorporation of synthetic long peptides (SLPs) in poly(lactic- co-glycolic acid) (PLGA) nanoparticles (NP) as a vaccine delivery vehicle. We showed that a low burst release of the encapsulated SLP was crucial to improve MHC class I presentation and $CD8^+$ T cell activation in comparison to soluble SLP (sSLP) *in vitro*. Using SLP-OVA24aa as vaccine antigen (Ag) and toll-like receptor (TLR) 2 ligand Pam3CSK4 as an adjuvant encapsulated in PLGA-NP (PLGA-SLP and PLGA-SLP/TLR2L), we show in this report that TLR 2 stimulation enhances MHC class I presentation of PLGA-SLP by dendritic cells (DCs), however co-encapsulation of the TLR ligand was not required for this effect. DC loaded with PLGA-SLP(/TLR2L) internalized NP into endo-lysosomal compartments and not the cytosol as occurs with sSLP. Moreover, PLGA-NP encapsulated SLP could be detected for prolonged periods inside endo-lysosomal compartments. Prolonged presence of NP inside DC resulted in MHC class I presentation of encapsulated SLP for up to 96 hr, which led to sustained $CD8^+$ T cell proliferation in *in vivo* adoptive transfer of PLGA-SLP loaded DC. These findings explain the *in vivo* effectiveness of nanoparticle vaccination and shows that PLGA-SLP is a promising delivery vehicle for clinical application as a cancer immunotherapy.

Keywords: Peptide antigen, synthetic long peptides, CTL epitope, PLGA nanoparticles, TLRL, cancer immunotherapy, cellular immune response

1. Introduction

Cancer immunotherapy is a promising treatment modality to enhance the tumor associated antigen (Ag) specific T cell responses in cancer patients. Efficient MHC class I Ag presentation and subsequent $CD8^+$ T cell priming are pre-requisites for optimal clinical efficacy of a cancer immunotherapy vaccine [1, 2]. We recently reported that synthetic long peptides (SLP) considerably facilitate MHC class I presentation in comparison to protein, which was related to faster uptake and processing of SLP by dendritic cells (DC) compared to that of protein Ag [3].

SLP-vaccines emulsified in Montanide(-ISA51) water-in-oil-in-water emulsion have been studied in the clinic against various forms of cancer [4, 5] and other immunological diseases [6, 7]. However, the use of Montanide is associated with considerable adverse effects [8-11]. In addition, montanide has poorly defined adjuvant properties and the release kinetics of the emulsified vaccine-Ag cannot be controlled. Alternative vaccine delivery systems and adjuvants for SLP, being at least as efficient as but having less side effects than Montanide, are therefore highly required like well-defined Toll like receptor ligands (TLRL). In light of this we have previously reported the succesful application of nanoparticles (NP) formulated with the fully biocompatible polymer, poly-(lactic-co-glycolic-acid) (PLGA) as delivery vehicle for SLP vaccines. Encapsulating SLP in PLGA led to a significant enhancement of MHC class I Ag presentation and $CD8^+$

T cell activation compared to soluble SLP [10]P. However, PLGA-NP have low immunostimulatory properties by itself but allows controled co-encapsulation and release of TLRL [12, 13].

The aim of the present paper was to study 1) how PLGA-NP encapsulated SLP is routed and processed into MHC class I molecules and 2) how a defined adjuvant co-encapsulated in NP affects the efficiency and duration of $CD8^+$ T cell activation by DC. For this purpose, NP were formulated together with a TLR2L (Pam3CSK4) as adjuvant, which effectively boosted vaccine-Ag specific immune responseswhen covalently conjugated to SLP [14, 15].

We show here that co-encapsulating TLR2L with SLP in PLGA-NP further enhances the efficiency of MHC class I cross-presentation of SLP by DC compared to plain PLGA-SLP. In addition, loading of DC using PLGA-NP results in sustained MHC class I presentation of SLP compared to soluble SLP. However, the effect of sustained MHC clas I presentation was not related to TLR2L-mediated DC maturation but likely because of the prolonged presence of PLGA-NP encapsulated SLP inside endo-lysosomal compartments upon uptake by DC. These organels are similar to the storage compartments in DC we have described for other antigen targeting system like FcR-mediated uptake [16].

Finally, we show that adoptive transfer of DC loaded with PLGA-SLP/TLR2L stimulated $CD8^+$ T cells over a sustained period of time whereas soluble SLP loaded DC failed to do so. Therefore, this study presents additional evidence for the use of PLGA-NP as a clinically suitable vaccine delivery systems to enhance direct MHC class I Ag presentation and T cell activation but also maintain $CD8^+$ T cell responses over a prolonged time period.

2. Material and methods

2.1. Mice

WT C57BL/6 (CD45.2/Thy1.2; H2-Kb) mice were obtained from Charles River Laboratories (France). TAP1 KO mice (C57BL/6 CD45.2/Thy1.2; H2-Kb) were purchased from the Jackson laboratory (Bar Harbor, ME). All mice were used at 8–12 weeks of age in accordance with national legislation and under supervision of the animal experimental committee of the University of Leiden.

2.2. Materials

The synthetic long peptide DEVSGLEQLESIINFEKLAAAAAK (SLP-OVA24) [17], covering the H2-Kb restricted $CD8^+$ T cell epitope SIINFEKL of ovalbumin (OVA) and SLP-OVA24-Bodipy-FL (Bp) were synthesized at the interdepartmental GMP facility of the Department of Clinical Pharmacy and Toxicology of Leiden University Medical Center as described previously [10]. Poly(D,L-lactic-co-glycolic acid) [PLGA], Resomer® RG 502H was purchased from Boehringer Ingelheim (Ingelheim, Germany). 4-(2-hydroxyethyl)-1-piperazine-ethanesulfonic acid (HEPES), dichloromethane (DCM), dimethyl sulfoxide (DMSO), and trifluoroacetic acid (TFA) were purchased from Sigma-Aldrich (Steinheim, Germany). Acetonitrile (ACN) and methanol (MeOH) were obtained from Biosolve BV (Valkenswaard, the Netherlands), Polyvinyl alcohol (PVA) 4-88 (31 kDa) was purchased from Fluka (Steinheim, Germany). Reversed phase HPLC column ReproSil-Pur C18-AQ 3 µm (150x4 mm) was purchased from Dr. Maisch HPLC GmbH (Ammerbuch-Entringen, Germany). Pam3CSK4 and Pam3CSK4-Rhodamine were purchased from Invivogen (San Diego, USA). Iscove's Modified Dulbecco's Medium (IMDM) was purchased from Lonza (Walkersville, USA). All other chemicals were of analytical grade and all aqueous solutions were prepared with milli Q water.

2.3. Nanoparticle preparation and characterization

Nanoparticles loaded with SLP-OVA24 were prepared using a double emulsion with solvent evaporation method as previously described [10]. In brief, 1.4 mg SLP-OVA24 were dissolved in 100 µL 50% ACN in 0.25 mM NaOH and then added to 400 µL 50 mM Hepes, pH 8.0. This solution was then added to 50 mg of PLGA in 1 ml of dichloromethane and the mixture was emulsified under sonication (30 s, 20 W). To this first emulsion (w1/o), 2 ml of an aqueous surfactant solution (for surfactant types, see results) were added immediately, and the mixture was emulsified again by sonication (30 s, 20 W), creating a double emulsion (w1/o/w2). The emulsion was then added drop-wise to 25 ml of extraction medium (0.3% w/v surfactant) previously heated to 40°C under agitation, to allow quick solvent evaporation, and left stirring for 1 h. The particles were then collected by centrifugation for 15 min at 15000 g at 10°C, washed, resuspended in Milli Q water, aliquoted and freeze-dried at -55°C in a Christ Alpha 1-2 freeze-drier (Osterode am Harz, Germany) overnight. For particles co-encapsulating SLP-OVA24 and Pam3CSK4, 250 µg of Pam3CSK4 were dissolved in DCM together with PLGA, and for particles containing SLP-OVA24-Bp-FL, circa 10% labeled peptide was added to the peptide solution.

Particle characterization was performed as described [10]. NP were diluted to 2.5 mg/ml in 1 mM Hepes pH 7.4. Size and polydispersity index (PDI) of NP were measured by dynamic light scattering, and zeta-potential was measured by laser Doppler electrophoresis, using a Zetasizer (Nano ZS, Malvern Ltd., United Kingdom). The encapsulation efficiency (EE) was calculated according to **equation 1** and drug loading (DL) by **equation 2**. EE of OVA24 was determined by measuring the peptide content

of digested particles by reversed phase HPLC as described [10]. EE of Pam3CSK4-Rhodamine was determined by measuring fluorescence detected in the supernatant against a calibration curve and expressed as percentage of the total amount added.

$$\%\,EE = \frac{\text{SLP/TLR2L mass in NP}}{\text{initial SLP/TLR2L mass}} \times 100 \quad (1)$$

$$\%\,DL = \frac{\text{encapsulated SLP/TLR2L mass}}{\text{total polymer} + \text{SLP/TLR2L mass}} \times 100 \quad (2)$$

2.4. Cells

Freshly isolated murine DCs were cultured from mouse bone marrow (BM) cells, as described before [18]. The D1 cell line, an immature primary splenic DC line (C57BL/6-derived), was cultured as described elsewhere [19]. B3Z $CD8^+$ T cells (H2-kb/SIINFEKL) are hybridoma cell lines expressing a β-galactosidase construct which upon T-cell activation can be measured by a colorimetric assay [3].

2.5. Murine MHC class I Ag presentation assays

C57BL/6 BMDCs or D1 cells (1*105 cells/well) were plated out in triplicate using 96-well plates (Greiner #655101) and incubated for 2.5 hr with the Ag at the indicated concentrations. Cells were washed 3x with complete medium to remove excess Ag before the B3Z $CD8^+$ T cells were added to assess MHC class I cross-presentation. T cells were cultured in the presence of Ag-loaded DC for 2.5 at 37 °C. In some experiments, BMDC or D1 cells were pre-incubated with epoxomicin (324800, Merck) or bafilomycin A1 (196000, Merck) followed by Ag-incubation as described above in the presence of the compounds. D1 cells were pre-incubated with bafilomycin A1 (196000, Merck) and MHC class I Ag presentation determined as described above. To study sustained MHC class I Ag presentation, 2*106 immature D1 cells were incubated for 2.5 hr with 4 μM SLP in different formulations. After incubation, cells were harvested and transferred to 50 ml Falcon tubes, resuspended in complete medium and centrifuged . This procedure was performed 3x to wash away unbound Ag. Cells were either used directly as Ag presentating cells (APC) (“direct condition”) or plated out again in petri dishes and further cultured for 96 hr (“chase condition”). Ag loaded D1 cells were then harvested and plated out in 96-wells plates (5*104 cells/well) and used as APC in co-culture with B3Z $CD8^+$ T cells to detect capacity to cross-present SLP in MHC class I molecules using a colorometric assay as described before [3].

2.6. Adoptive transfer of Ag loaded DC

C57BL/6 BMDC cells (10*106 cells/petri dish, Corning # 430589) were loaded with 4 μM PLGA-SLP, PLGA-SLP/TLR2L and sSLP on t = - 96 hr and t = -2.5 hr. Cells were washed to remove unbound Ag and either used directly or further cultures in the absence of Ag. On t = - 1 day, splenocytes from Thy1.1$^+$ OT-I mice were harvested and transferred i.v. to recipient animals (10*106 splenocytes/mouse). On t = 0, OVA-specific T cells enriched mice received i.v. 1*106 DC loaded with PLGA-SLP, PLGA-SLP/TLR2L. Tail vein bloodsamples were collected on t = day 3 post-transfer of DC and analyzed for the percentages of Thy1.1$^+$ CD8$^+$ T cells using rat anti-mouse CD90.1-APC, CD3-AF800 and CD8-FITC antibodies (Biolegend). Samples were measured using an LSRII flow cytometer (BD) and analyzed with FlowJo software (Treestar).

2.7. Confocal microscopy

DCs were incubated for 24 hr with 10 μM SLP-OVA24-Bodipy-FL in different formulations at 37°C. Specific murine DC used is described in the figure legends. After incubation cells were washed 3 times to remove excess and unbound Ag, resuspended at a concentration of 2x105 cells in 200 μl complete medium and plated into poly-d-lysine coated glass-bottom dishes (MatTek) followed by mild centrifugation to allow the cells to adhere. Adhered cells were then fixed with 0.2% paraformaldehyde. All imaging experiments were carried out on a Leica TCS SP5 confocal microscope (HCX PL APO 63×/1.4 NA oil-immersion objective, 12 bit resolution, 1024×1024 pixels, pinhole 2.1 Airy discs, zoom factor 1 or 7). Imaging was performed using the 488 nm line from an Argon laser collecting emission between 500 and 600 nm. Dual color images were acquired by sequential scanning, with only one laser per scan to avoid cross talk. The images were analyzed using the Leica software program (LAS AF).

2.8. Analysis of cytokine production by DC using Enzyme-linked Immunosorbent Assay (ELISA)

BMDC were incubated for 24 hr with NP. Supernatants were harvested and tested for IL-12 p70 (BD OptEIA™ MOUSE IL-12 Cat. Nr 555256) following manufacturer's instructions.

2.9. Statistics

Graphpad prism was used as the main statistical software. Statistical analyses applied to determine the significance of differences are described in the figure legends.

3. Results

3.1. Characterization of formulated PLGA-SLP and PLGA-SLP/TLR2L NP

PLGA-NP were formulated using a modified double emulsion method and solvent evaporation technique with SLP-OVA24 as described before, PLGA-SLP [10]. This formulation was adapted by adding the TLR2 ligand (TLR2L) Pam3CSK4 in the organic phase to yield PLGA-NP co-encapsulating SLP and adjuvant, PLGA-SLP/TLR2L. For visualization purposes selected batches were formulated with 10 % SLP-OVA24-Bodipy-FL (SLP-Bp). Fluorescent SLP was added during formulation. Particle characteristics are described in **Table 1**.

Co-encapsulation of TLR2L and/or SLP-Bp did not affect the physical properties of the formulated NP, with several batches showing very similar characteristics (**Table 1**).

Table 1: Characterization of PLGA-SLP/TLR2L NP

Formulation	%DL SLP^{o}	%EE SLP^{o}	%DL Pam3CSK4	%EE Pam3CSK4	Size (nm)	PDI	ZP (mV)
PLGA-SLP*	1.06 ± 0.15	39 ± 6	n/a	n/a	322 ± 44	0.19 ± 0.04	-12 ± 1
PLGA-SLP/ TLR2L*	1.02 ± 0.17	38 ± 6	0.32 ± 0.05	67 ± 10	293 ± 19	0.18 ± 0.04	-13 ±1
PLGA-SLP-Bp**	1.01	37	n/a	n/a	312	0.23	-16
PLGA-SLP/ TLR2L-BP**	0.95	35	0.16	33	304	0.20	-13

DL = drug loading; EE = encapsulation efficiency; PDI = poly dispersity index; variance, an arbitrary measure for the degree of dispersity in particle size within one batch of particles suspension, PDI values below 0.3 was considered monodisperse and accepted for follow up studies [20].ZP = zeta potential; The magnitude of the zeta potential is predictive of the colloidal stability. Nanoparticles with Zeta Potential values greater than $^{+}$25 mV or less than -25 mV typically have high degrees of stability. Dispersions with a low zeta potential value will eventually aggregate due to Van der Waal inter-particle attractions.

^{o}SLP-OVA24 (DEVSGLEQLESIINFEKLAAAAAK).

*Values represent average ±SD of > 4 independently prepared batches.

**Values obtained from 1 batch.

3.2. Enhanced cross-presentation of PLGA-NP encapsulated SLP in the presence of TLR2L

DC loaded with PLGA-SLP cross-presented SLP in the context of MHC class I molecules with higher efficiency compared to sSLP, as published previously [20]. TLR-stimulation is known to improve proteasome activity and thus enhance MHC class I Ag cross-presentation. Indeed, the presence of TLR2L during Ag-loading enhanced MHC class I cross-presentation of all SLP-formulations tested compared to DC loaded in the absence of TLR2L (**Figure 1A**). PLGA-SLP/TLR2L resulted in better $CD8^+$ T cell activation than PLGA-SLP. However, co-encapsulation of TLR2L was dispensable to enhance MHC class I presentation of PLGA-encapsulated SLP *in vitro* as mixtures of PLGA-SLP $^+$ soluble TLR2L (sTLR2L) showed similar potency to PLGA-SLP/TLR2L.

TLR2 stimulation failed to improve the cross-presentation of sSLP to comparable levels as observed with PLGA-encapsulated SLP (**Figure 1A**). This observation stresses the importance of an optimal delivery method to achieve high levels of Ag intracellularly and to improve MHC class I Ag processing.

In summary, combining TLR2L stimulation with PLGA-NP delivery of SLP significantly improves MHC class I presentation compared to Ag loading in the absence of TLR2L. The positive effect of TLR2L was irrespective of co-encapsulation in PLGA-NP.

3.3. Ag-delivery via PLGA-NP results in prolonged MHC class I Ag cross-presentation

The duration of MHC class I presentation and TCR recognition/binding is an important factor determining $CD8^+$ T cell priming. Short TCR-stimulation leads to sub-optimal T cell priming which is associated in impaired effector functions anergy [21, 22]. The long term effects on MHC class I cross-presentation of SLP was studied by stimulating B3Z $CD8^+$ T cells with 96 hr rested Ag-loaded DC. DC were incubated for 2.5 hr in the presence of 4 μM SLP in either soluble or particulate form with or without TLR2L. As a positive control, DC were incubated with SLP-TLR2L conjugates which induce the formation of Ag-storage compartments upon internalization. These compartments facilitate prolonged MHC class I presentation and sustained $CD8^+$ T cell priming as we have previously reported [14, 18]. DC loaded with sSLP failed to activate $CD8^+$ T cells 96 hr post Ag-incubation (**Figure 1B**). Only DC incubated with PLGA-encapsulated Ag and the SLP-TLR2L conjugate were capable of MHC class I SLP cross-presentation after 96 hr (**Figure 1B**).

TLR-stimulation has been shown to slow down the decay of MHC class I molecules thereby prolonging cell-surface expression of MHC class I molecule/peptide complexes

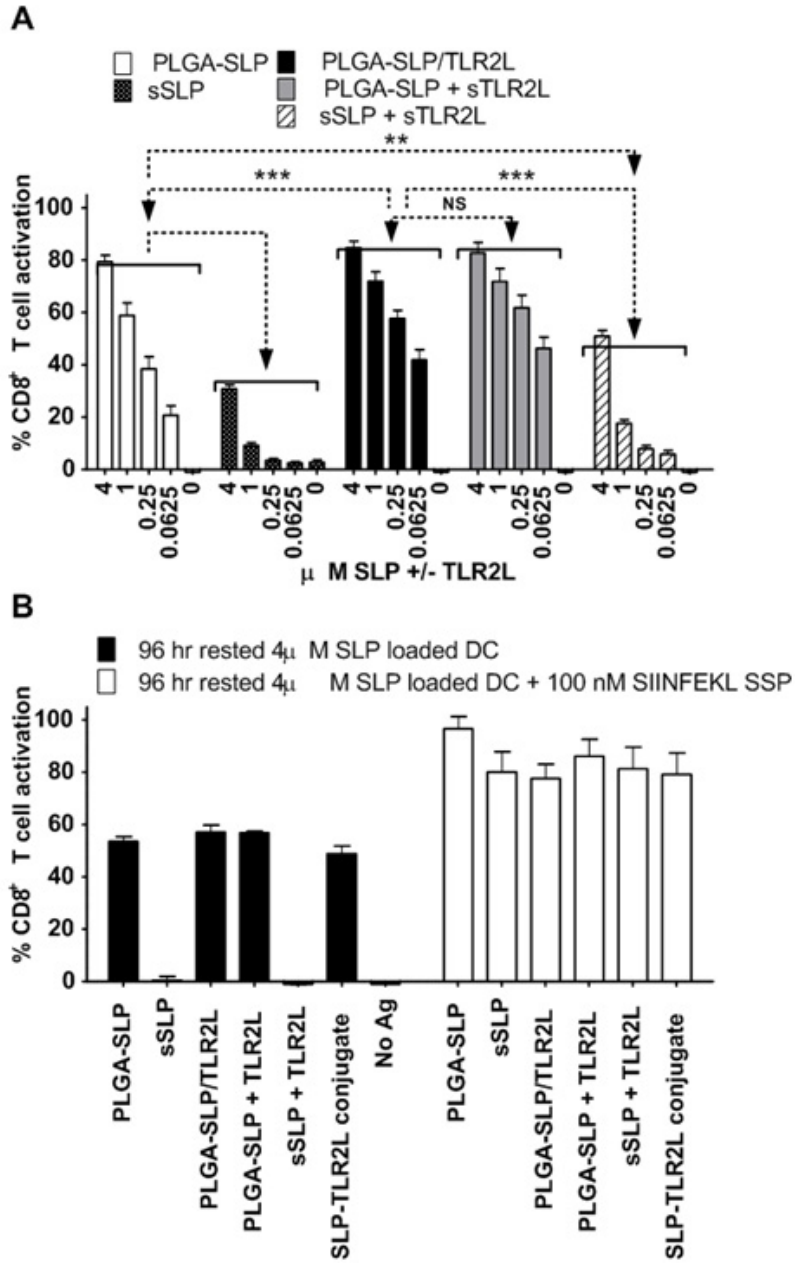

Figure 1. TLR2 stimulation improves MHC class I cross-presentation of PLGA-NP encapsulated SLP. D1 cells were incubated for 2.5 h with titrated amounts of SLP-OVA24 in different formulations with our without Pam3CSK4 (TLR2L) and co-cultured overnight in the presence of **(A)** B3Z CD8+ T cells. T-cell activation was determined as described in Materials and methods. **(B)** D1 cells were incubated with 4 μM Ag for 2.5 hr on t = -96 hr (chase) and on t = -2.5 hr (direct). "Chase" and "direct" Ag loaded DC were harvested at t = 0 hr and their APC capacity to activate B3Z CD8+ T cells compared. Data are shown as mean + SD of three samples from one representative experiment representative of four (A) and three (B) experiments performed. *** $P < 0.001$ using a two-way ANOVA and Bonferroni posttests.

[23]. In our system however, prolonged presence of MHC class I molecules/peptide complexes is unlikely to be the main mechanism facilitating sustained CD8+ T cell activation by PLGA-SLP as plain particles in the absence of additional adjuvants poorly matured DC. PLGA-SLP had no phenotypical (**Figure 2A**) nor functional DC maturating effects (**Figure 2B**) on DC. Addition of Pam3CSK4 to PLGA-SLP formulations, to obtain PLGA-SLP/TLR2L, very efficiciently matured DC (**Figure 2**). However, TLR2L stimulation did not further MHC class I Ag cross-presentation by DC loaded with PLGA-SLP or sSLP loaded DC and then rested for 96 hr in culture in the absence of Ag. Therefore, TLR2-stimulation by itself cannot explain our observations of prolonged Ag presentation by DC pulsed by PLGA-SLP.

In conclusion, Ag delivery via PLGA-NP results in prolonged MHC class I presentation *in vitro* and sustained CD8+ T cell activation. Prolonged MHC class I presentation of SLP was not dependent on DC maturation.

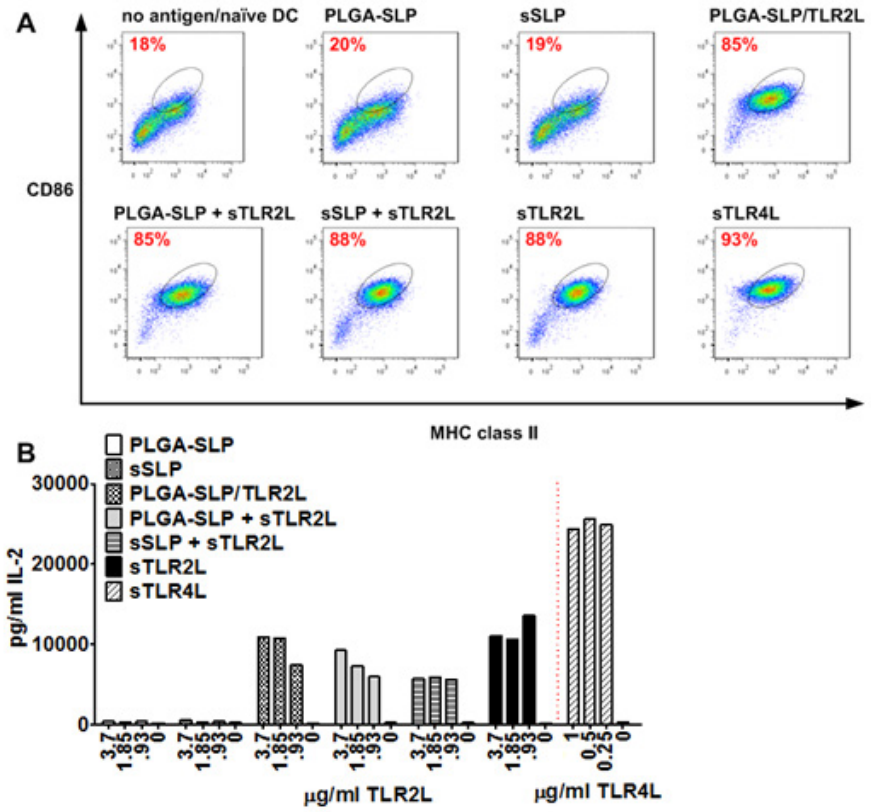

Figure 2. Addition of TLR2L to plain PLGA-SLP and sSLP improves adjuvanticity and results in DC maturation. D1 cells were incubated in the presence of titrated amounts of SLP formulations with or without Pam3CSK4 (Invivogen, tlrl-pms), and soluble LPS (TLR4L) (Sigma L4130, Escherichia coli 0111:B4). After 24 hr supernatants were collected, DC harvested and stained for MHC class II and CD86 and their expression analyzed by FACS **(A)**. Percentages indicate the numbers of double positive cells. Supernatants were analyzed via ELISA for IL-2 levels **(B)**. Data shown are representative of three independent experiments.

3.4. DC loaded with SLP encapsulated in NP are capable of sustained *in vivo* priming after adoptive transfer

The *in vitro* observations were confirmed *in vivo* by transferring DC which were loaded with Ag on t = -96 hr into recipient mice enriched with OT-I CD8⁺ T cells on day before adoptive transfer. The extent of CD8⁺ T cell expansion was compared to mice receiving DC loaded with Ag (-2.5 hr, "direct").

Only DC which were loaded with PLGA-SLP or PLGA-SLP/TLR2L induced significant OT-I CD8⁺ T expansion using freshly Ag-loaded DC (**Figure 3**). DC loaded with sSLP performed poorly as APC at the concentrations of sSLP tested. Poor priming of OT-I CD8⁺ T cells can be related to the lower MHC class I presentation of sSLP compared to PLGA-SLP but is most likely a result of sub-optimal activation of naive OT-I CD8⁺ T cells, which are co-stimulation dependent, by sSLP loaded DC which have a immature phenotype (**Figure 2**). PLGA-SLP and even PLGA-NP in general, do not mature DC. However NP-based Ag delivery is very efficient leading to high density of Ag-epitope loaded MHC class I molecules on the cell-surface leading to sufficient triggering of OT-I CD8⁺ T cells for them to proliferate *in vivo*. PLGA-SLP with co-encapsulated TLR2L results in significant OT-I expansion even after 96 hrs incubation indicating sustained antigen storage of the particle-delivered antigen by DC.

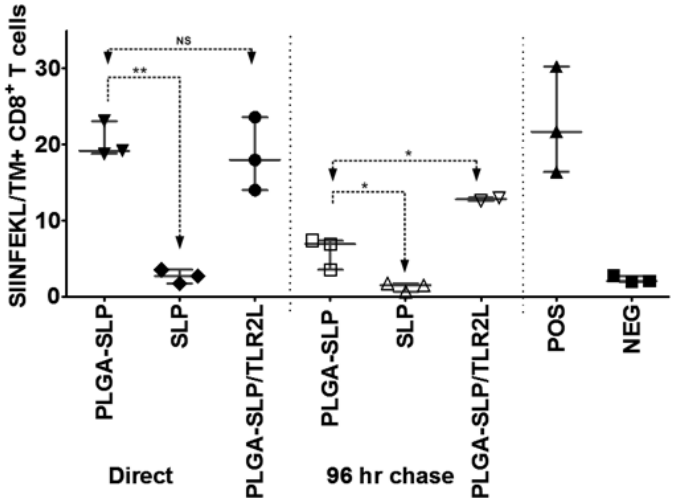

Figure 3. PLGA-SLP loaded DC possesses APC capacity and stimulated CD8⁺ T cells 96 hr after Ag-loading. Ag loaded BMDC (C57BL/6) were tested for their capacity to expand specific CD8⁺ T cells *in vivo*. WT C57BL/6 animals received 10*106 OVA-specific Thy1.1⁺ OT-I splenocytes i.v. on t = day -1. On t = 0, OVA-specific T cell enriched mice received i.v. 1*106 DC loaded with PLGA-SLP, PLGA-SLP/TLR2L and sSLP on t = -96 hr and t = -2.5 hr. Blood samples were taken on t = day 3 post-transfer of DC and analyzed for the percentages of Thy1.1⁺CD8⁺ T cells. DC loaded with SIINFEKL and 10 µg/ml LPS and antigen naïve DC were used as positive (pos) and negative (neg) control. Percentages determined for each individual mice are displayed and data shown are representative of one independent experiments. *P< 0.05 using a unpaired student t-test.

3.5. Re-routing and prolonged presence of SLP into the endosomes by encapsulation in PLGA-NP

We analyzed if the intracellular localisation of PLGA-SLP after uptake by DC might play a role in the observed MHC class I presentation. For this purpose DC were incubated with sSLP, PLGA-SLP and PLGA-SLP/TLR2L and analyzed directly by confocal microscope. D1 dendritic cells and BMDC were highly capable to internalizing Bp-labeled SLP in the tested formulations (green fluorescence, **Figures 4 & 5**).

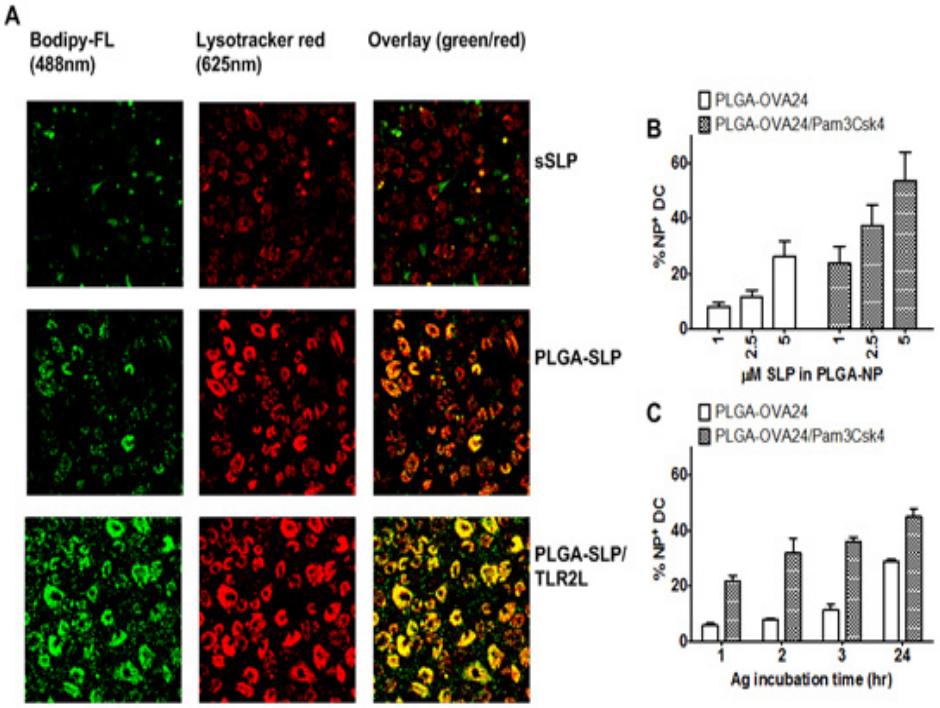

Figure 4. Rerouting of SLP into endo-lysosomal compartments upon encapsulation of in PLGA-NP. BMDC were incubated with 20 µM sSLP-Bp, 20 µM PLGA-SLP-Bp (10% SLP-Bodipy-FL) or 20 µM PLGA-SLP-Bp/TLR2L (10% SLP-Bodipy-FL) (excitation- 488nm, visualized as the green signal) for 2.5 hr and co-stained with Lysotracker red for visualization of the endo-lysosomes (red signal) and visualized by confocal microscopy. **(A)** 1st column shows images depicting green signal as the fluorescence of Bodipy-FL (488nm). 2nd column shows images depicting red signal as the fluoresence of the lysotracker red/endo-lysosomes (625nm). 3rd column depicts overlay images of red/green. Yellow-overlay signal marks co-localization. Images were analyzed using Leica software. BMDC were incubated at 4°C and 37°C with **(B)** titrated amounts of PLGA-SLP, PLGA-SLP/TLR2L and PLGA-SLP + sTLR2L (10% SLP-Bodipy-FL). (C) Alternatively, DC were incubated with with 2.5 µM of PLGA-SLP and PLGA-SLP/TLR2L (10% SLP-Bodipy-FL). Ag uptake was quantified by flow cytometry and data shown are absolute values (% NP^+ DC at 37°C - % NP^+ DC at 4°C) and represent Avg + SEM of 3 independent experiments (A) and Avg + SD of 2 independent experiments.

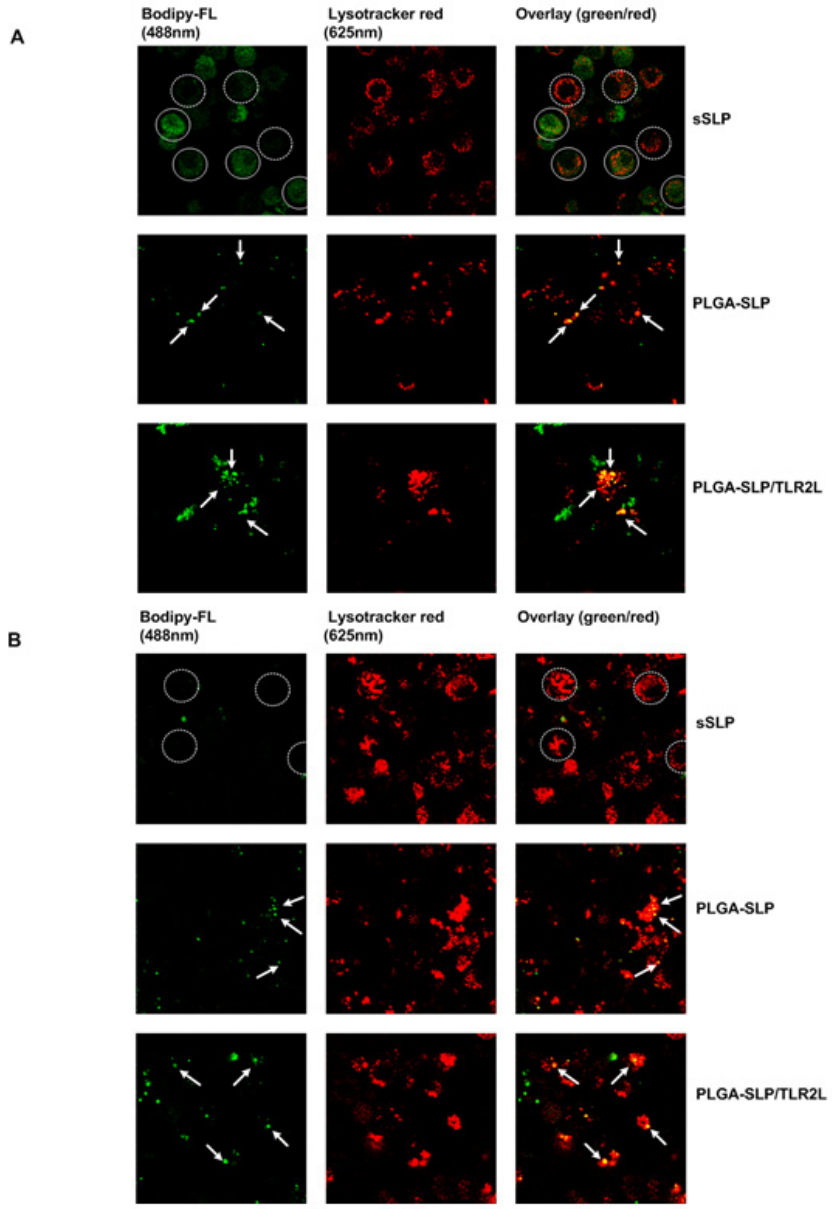

Figure 5. Sustained presence of PLGA-NP encapsulated SLP in endo-lysosomes. D1 cells were incubated with 20 µM sSLP-Bp, 20 µM PLGA-SLP-Bp (10% SLP-Bodipy-FL) or 20 µM PLGA-SLP-Bp/TLR2L (10% SLP-Bodipy-FL) (488nm) for 2.5 hr on t = - 2.5 h **(A)** and t = - 96 h **(B)** and co-stained with Lysotracker red for visualization of the endo-lysosomes on t = - 15 min. Live cell imaging were performed at t = 0. 1st column shows images depicting green signal as the fluorescence of Bodipy-FL (488nm). 2nd column shows images depicting red signal as the fluoresence of the lysotracker red/endo-lysosomes (625nm). 3rd column depicts overlay images of red/green. White arrow indicates hotspots (yellow) within a cell were green and red co-localize. Closed circles show cells containing green-flourescent signal (and red fluorescent signal). Dashed circles depict cells containing only red fluorescent signals. Images were analyzed using Leica software.

sSLP internalized by DC was present for a large part outside the endo-lysomes as we showed before [20] whereas PLGA-encapsulated SLP showed high co-localization, with endo-lysomes, suggested by the formation of bright yellow spots, marked in the **Figures 4 & 5** by the arrows. DC which took up NP tend to have larger endo-lysosomal compartments (bright red spots, **Figures 4 & 5**) compared to DC which internalized sSLP which might suggest formation of phagolysosomes. The results indicate that encapsulation of SLP inside PLGA-SLP modulates intracellular trafficking of SLP by keeping the Ag inside endosomal compartments, thereby directing it away from the cytosol.

Brighter yellow spots were observed when BMDC internalized PLGA-SLP in comparison to sSLP. This suggest that DC take up much higher amounts of SLP on a single cell basis when it is encapsulated in PLGA-NP, pointing to the more efficient uptake by DC of SLP when encapsulated (**Figure 4**). Interestingly, encapsulation of TLR2L in PLGA-NP (PLGA-SLP/TLR2L) even further enhanced the efficiency (**Figure 4B**) and rapidity of NP internalization (**Figure 4C**) by BMDC suggesting an additional role for TLR2 in the internalization of NP.

DC are known to preserve internalized PLGA-(micro)spheres inside endo-lysosomal compartments for up to 48 hr [25] which suggests that intracellular hydrolysis of PLGA particles to be a slow process. In our study, sustained MHC class I cross-presentation of PLGA-encapsulated SLP could be detected even after 96 hr. We therefore analyzed D1 cells loaded with sSLP, PLGA-SLP, PLGA-SLP/TLR2L directly after loading (**Figure 5A**) or after 96 hr rest (**Figure 5B**). sSLP-loaded D1 cells analyzed after 96 hr rest showed clear differences with DC analyzed directly after Ag-loading. Fluorescent signal of SLP was largely undetectable in DC cultured with sSLP whereas labeled SLP originated from the PLGA-SLP or PLGA-SLP/TLR2L could be clearly detected still inside endosomal compartments (**Figure 5**).

It is known that internalized soluble proteins are also routed into endosomal compartments [24-26]. However, endosomal presence of an Ag does not guarantee preservation as soluble protein was not detected inside DC after 96 hr (**Supplemental Figure 1**). This observation fits with our previous reports showing that soluble proteins do not lead to sustained Ag presentation [18].

3.6. Processing of PLGA-NP encapsulated SLP can be blocked by inhibitors of endo-lysosomal acidification, proteasome and TAP

Exogenous Ag routed towards the MHC class I cross-presentation pathway can follow two pathways I) the classical cytosolic pathway or II) the endosomal pathway [27-29]. The endosomal pathway is dependent on the pH inside the endo-lysosomes but the cytosolic pathway is (mostly) independent of the pH gradient inside endo-lysosomes [29]. We observed that $CD8^+$ T cell activation by DC loaded with PLGA-SLP and PLGA-SLP/TLR2L can be completely blocked (**Figure 6**) in a dose dependent manner

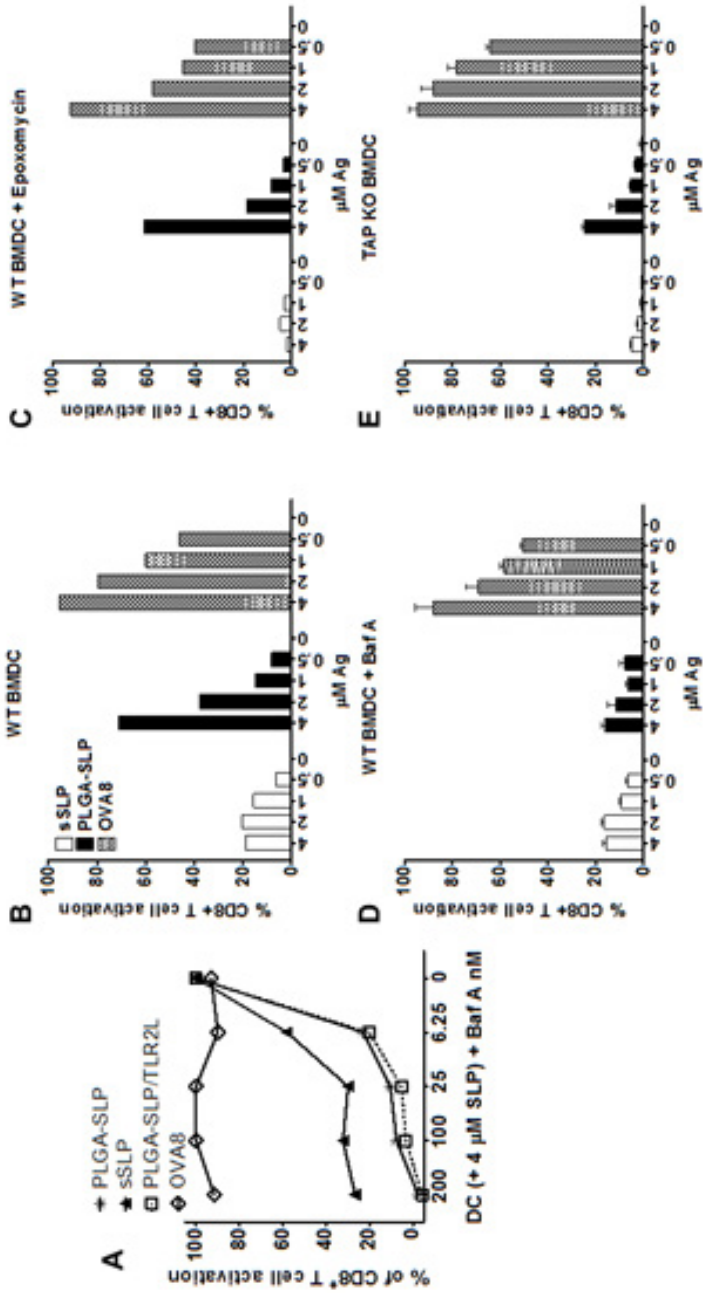

Figure 6. MHC class I cross-presentation PLGA-SLP and PLGA-SLP/TLR2L is impaired in the absence of functional proteasome, TAP and when endo-lysosomal acidification is inhibitedBafilomycin A). D1 cells were pre-incubated with indicated titrated concentrations of bafilomycin A1 (196000, Merck) followed by culture in the presence of 4 µM sSLP, PLGA-SLP, PLGA-SLP/TLR2L and 5 nM SSP-OVA8aa (SIINFEKL). Cells were washed 3x times with complete medium before the B3Z $CD8^+$T-cells were added followed by O/N incubation at 37°C. **(B)** WT BMDC were incubated with titrated amounts of sSLP or PLGA-SLP without additional treatments or in the presence of **(C)** epoxomycin or (E) Bafilomycin A. (D) TAP KO BMDC were incubated with titrated amounts of sSLP or PLGA-SLP.

using the lysotropic agent, bafilomycin A (Baf A). MHC class I cross-presentation of sSLP was slightly decreased as observed before [3] but $CD8^+$ T cell activation could still be detected at the highest concentration of the compound tested in this study. The presentation of the minimal MHC class I binding peptide (OVA8) was unaffected over the whole range of concentrations used. PLGA-SLP MHC class I cross-presentation was reduced in the presence of a proteasome inhibitor (**Figure 6B & C**). MHC class I processing of PLGA-SLP was significantly impaired in the absence of functional TAP (**Figure 6B & E**) or when when endo-lysozomal acidification is blocked (**Figure 6B & D**).

4. Discussion

In this study, we analyzed the effects on MHC class I presentation of co-encapsulating a TLR2L with SLP in PLGA-NP. SLP and PLGA-NP are inert synthetic materials with poor immunestimulating properties. The therapeutic effectivity of cancer vaccines is largely based on its potency to activate DCs, which have superiour capacity to induce robust anti-tumor T cell responses.

We previously reported the succesful formulation of PLGA-SLP using a novel double emulsion and solvent-evaporation technique. Applying PLGA-NP as a vaccine delivery system, the efficacy of MHC class I Ag presentation and subsequent $CD8^+$ T cell activation by DCs was significantly enhanced [10] compared to sSLP. We have also shown recently that plain PLGA-NP have poor DC activating properties compared to TLRL [12]. With the purpose of further increasing the vaccine potency of PLGA-SLP, we have included a TLR2L, Pam3CSK4; an adjuvant which has led to promising pre-clinical results when covalently coupled to SLP. To this end, TLR2L was co-encapsulated in PLGA-NP with the goal to achieve asubstantial DC activation leadingleads to better $CD8^+$ T cell activation in comparison to particles which are not adjuvanted.

In light of our recent findings showing that sSLP are efficiently cross-presented because of a rapid translocation into the cytosol facilatating proteasome dependent processing; the intracellular location of PLGA-SLP was studied to elucidate if PLGA-NP further enhances translocation of SLP, after release from the NP, to the cytosol or if different mechanisms are involved in the handling of PLGA-encapsulated SLP in comparison to the sSLP.

We show here that the addition of Pam3CSK4 to PLGA-NP encapsulating SLP strongly promotes DC maturation and $CD8^+$ T cell activation. The difference on Ag uptake and MHC class I cross-presentation of PLGA-SLP versus PLGA-SLP/TLR2L was was max 3-fold. Lower than we expected given our previous studies using SLP-TLR2L [14]. This moderate enhancement can be explained considering the already very efficient uptake, processing and presentation of plain PLGA-SLP (NP) by DC which perhaps is already close to maximum levels.

Moreover, Pam3CSK4 was not to required to be encapsulated inside particles for it to exert its positive effects on MHC class I presentation of SLP. Mixing sTLR2L with plain PLGA-SLP led to similar results as using PLGA-SLP/TLR2L. Thus Pam3CSK4 has a different effect on the potency of SLP when co-encapsulated in NP compared to covalently coupling the compound to a peptide, which results in very strong enhancement of $CD8^+$ T cell activation compared to mixtures of SLP and Pam3CSK4 [14].

Pam3CSK4 has a lipidic nature and contains positively charged lysine residues which direct adsorbtion to to the negatively charged PLGA-NP surface due to hydrophobic and (or) electrostatic interactions [3]. The adsorbtion of Pam3CSK4 to PLGA-SLP when mixed might lead to similar NP-characteristics as PLGA-SLP/TLR2L. This effect could explain why both the mixing or co-encapsulation will result in an similar participation of Pam3CSK4 in MHC class I presentation. In conclusion, we show that addition of a Pam3CSK4, whether co-encapsulated or not, further improves MHC class I cross-presentation of SLP and improves $CD8^+$ T cell activation compared to plain PLGA-SLP.

sSLP present in the cytosol are degraded via ubiquitin proteasome system (UPS) [30], whereas the Ag present inside endo-lysosomal compartments can be protected from rapid degradation by the UPS. Upon internalization of PLGA-NP by DC, a majority of the Ag could be detected inside the endo-lysosomes where hydrolysis of the polymer takes place releasing the encapsulated SLP [31]. Thus, the PLGA-NP encapsulated Ag inside endo-lysosomal compartments (**Figure 4**) serves as an intracellular reservoir which gradually releases the SLP for processing via the classical proteasome-TAP dependent MHC class I processing pathways. Baf A clearly interferes with MHC class I Ag presentation of PLGA-SLP. One possibility is that the compound blocks the transportation of SLP from the endo-lysosomes to the cytosol [32]. Another possibility is that Baf A modulates the activity of endo-lysosomal cathepsins [31]. Cathepsin S has been shown to have a role in MHC class I cross-presentation [27]. Using BMDC generated from Cathepsin S KO mice, we did not observe differences in MHC class I cross-presentation of PLGA-SLP compared to WT BMDC (data not shown). Taken our results using proteasome inhibitors and TAP-deficient BMDC we show that SLP encapsulated in PLGA-NP is cross-presented via the classical MHC class I processing pathway but we cannot exclude that the endo-lysosomal environment and other pH dependent proteases still play a role in the observed MHC class I Ag cross-presentation [28, 29].

The most important observation of this study was that encapsulation of sSLP in PLGA-NP results in sustained presence of the Ag inside DC upon internalization. More over, DC loaded with PLGA-SLP or PLGA-SLP/TLR2L showed prolonged MHC class I presentation in comparison to DC loaded with sSLP. Prolonged Ag presentation was not dependent on TLR2L stimulation but the addition of Pam3CSK4 does improve and sustain $CD8^+$ T cell activation over a longer time period *in vivo*. Others observed similar results using PLGA-particles encapsulating proteins [33]. However, in contrast to our results, it has been reported that PLGA-particles induce membrane rupture and rapid endo-lysosomal [34] followed by “leakage” of the PLGA-encapsulated Ag inside the cytosol; so called endosomal escape [33]. Membrane rupture by particulate Ag is

associated with inflammasome activation and secretion of IL-1β by APC [35]. In our system, however we could not detect IL-1β in culture supernatants using ELISA after 24 hr incubations of DC with PLGA-SLP nor PLGA-SLP/TLR2L (data not shown). As mentioned before, we could detect green-fluorescent signal of the SLP-OVA24-Bodipy-FL and $CD8^+$ T cell activation even after 96 hr indicating that in our study the majority of PLGA-encapsulated SLP was not directly tranported to the cytosol after DC internalized the NP. Thus, internalized PLGA-NP show functional similarities with intracullar storage compartments as reported for other targeted vaccine delivery systems [14, 18].

Therefore, we postulate that the efficient and prolonged MHC class I presentation observed using PLGA-SLP and PLGA-SLP/TLR2L is related to preservation of the Ag inside intact intracellular compartments. We show here based on the intracellular localization of internalized PLGA-NP and functional studies that these particles also end up in Ag storage compartments [18].

Finally, direct s.c. vaccinations with PLGA-SLP/TLR2L but not PLGA-SLP induces endogenous Ag-specific $CD8^+$ T cells capable of target cell lysis (**Supplemental Figure 2**). In conclusion, the study reported here supports a mechanism that $CD8^+$ T cell responses is enhanced when the Ag is cross-presented in MHC class I molecules in a sustained manner. We show that the co-encapsulation of a TLR2L further boosts these effects and thus supports the use of PLGA-NP co-encapsulating long peptide vaccines and adjuvants as an anti-cancer vaccine. Cancer cells are notorious for providing very few “danger signals”, which is one of the causes why the immune system sometimes fails to clear cancers. However, if one vaccinates with PLGA-SLP/TLR2L, encoding tumor associated Ag (TAA), for example the sustained release of Ag and adjuvant will lead to strong DC maturation, enhanced and prolonged MHC class I presentation and efficient priming of cytotoxic $CD8^+$ T cells. Indeed, vaccination with PLGA-NP based vaccines results in robust anti-tumor responses with the capacity to significantly control tumor out growth [36-39].

5. References

1. Flinsenberg, T.W., E.B. Compeer, J.J. Boelens, and M. Boes, Antigen cross-presentation: extending recent laboratory findings to therapeutic intervention. Clin Exp Immunol, 2011. 165(1): p. 8-18.
2. Melief, C.J., Cancer immunotherapy by dendritic cells. Immunity, 2008. 29(3): p. 372-83.
3. Rosalia, R.A., E.D. Quakkelaar, A. Redeker, S. Khan, M. Camps, J.W. Drijfhout, A.L. Silva, W. Jiskoot, T. van Hall, P.A. van Veelen, G. Janssen, K. Franken, L.J. Cruz, A. Tromp, J. Oostendorp, S.H. van der Burg, F. Ossendorp, and C.J. Melief, Dendritic cells process synthetic long peptides better than whole protein, improving antigen presentation and T-cell activation. Eur J Immunol, 2013. 43(10): p. 2554-65.
4. Sabbatini, P., T. Tsuji, L. Ferran, E. Ritter, C. Sedrak, K. Tuballes, A.A. Jungbluth, G. Ritter, C. Aghajanian, K. Bell-McGuinn, M.L. Hensley, J. Konner, W. Tew, D.R. Spriggs, E.W. Hoffman, R. Venhaus, L. Pan, A.M. Salazar, C.M. Diefenbach, L.J. Old, and S. Gnjatic, Phase I trial of overlapping long peptides from a tumor self-antigen and poly-ICLC shows rapid induction of integrated immune response in ovarian cancer patients. Clin Cancer Res, 2012. 18(23): p. 6497-508.
5. Kenter, G.G., M.J. Welters, A.R. Valentijn, M.J. Lowik, D.M. Berends-van der Meer, A.P. Vloon, F. Essahsah, L.M. Fathers, R. Offringa, J.W. Drijfhout, A.R. Wafelman, J. Oostendorp, G.J. Fleuren, S.H. van der Burg, and C.J. Melief, Vaccination against HPV-16 oncoproteins for vulvar intraepithelial neoplasia. N Engl J Med, 2009. 361(19): p. 1838-47.
6. Park, H., L. Adamson, T. Ha, K. Mullen, S.I. Hagen, A. Nogueron, A.W. Sylwester, M.K. Axthelm, A. Legasse, M. Piatak, Jr., J.D. Lifson, J.M. McElrath, L.J. Picker, and R.A. Seder, Polyinosinic-polycytidylic acid is the most effective TLR adjuvant for SIV Gag protein-induced T cell responses in nonhuman primates. J Immunol, 2013. 190(8): p. 4103-15.
7. Jarvi, S.I., D. Hu, K. Misajon, B.A. Coller, T. Wong, and M.M. Lieberman, Vaccination of captive nene (Branta sandvicensis) against West Nile virus using a protein-based vaccine (WN-80E). J Wildl Dis, 2013. 49(1): p. 152-6.
8. Leenaars, P.P., M.A. Koedam, P.W. Wester, V. Baumans, E. Claassen, and C.F. Hendriksen, Assessment of side effects induced by injection of different adjuvant/antigen combinations in rabbits and mice. Lab Anim, 1998. 32(4): p. 387-406.
9. Aucouturier, J., L. Dupuis, S. Deville, S. Ascarateil, and V. Ganne, Montanide ISA 720 and 51: a new generation of water in oil emulsions as adjuvants for human vaccines. Expert Rev Vaccines, 2002. 1(1): p. 111-8.
10. Silva, A.L., R.A. Rosalia, A. Sazak, M.G. Carstens, F. Ossendorp, J. Oostendorp, and W. Jiskoot, Optimization of encapsulation of a synthetic long peptide in PLGA nanoparticles: low-burst release is crucial for efficient CD8(+) T cell activation. Eur J Pharm Biopharm, 2013. 83(3): p. 338-45.
11. Aucouturier, J., S. Ascarateil, and L. Dupuis, The use of oil adjuvants in

therapeutic vaccines. Vaccine, 2006. 24 Suppl 2: p. S2-44-5.
12. Rosalia, R.A., A.L. Silva, M. Camps, A. Allam, W. Jiskoot, S.H. van der Burg, F. Ossendorp, and J. Oostendorp, Efficient ex vivo induction of T cells with potent anti-tumor activity by protein antigen encapsulated in nanoparticles. Cancer Immunol Immunother, 2013. 62(7): p. 1161-73.
13. Yoshida, M., J. Mata, and J.E. Babensee, Effect of poly(lactic-co-glycolic acid) contact on maturation of murine bone marrow-derived dendritic cells. J Biomed Mater Res A, 2007. 80(1): p. 7-12.
14. Khan, S., M.S. Bijker, J.J. Weterings, H.J. Tanke, G.J. Adema, T. van Hall, J.W. Drijfhout, C.J. Melief, H.S. Overkleeft, G.A. van der Marel, D.V. Filippov, S.H. van der Burg, and F. Ossendorp, Distinct uptake mechanisms but similar intracellular processing of two different toll-like receptor ligand-peptide conjugates in dendritic cells. J Biol Chem, 2007. 282(29): p. 21145-59.
15. Zom, G.G., S. Khan, D.V. Filippov, and F. Ossendorp, TLR ligand-peptide conjugate vaccines: toward clinical application. Adv Immunol, 2012. 114: p. 177-201.
16. van Montfoort, N., P.A. t Hoen, S.M. Mangsbo, M.G. Camps, P. Boross, C.J. Melief, F. Ossendorp, and J.S. Verbeek, Fcgamma receptor IIb strongly regulates Fcgamma receptor-facilitated T cell activation by dendritic cells. J Immunol, 2012. 189(1): p. 92-101.
17. Feltkamp, M.C., G.R. Vreugdenhil, M.P. Vierboom, E. Ras, S.H. van der Burg, J. ter Schegget, C.J. Melief, and W.M. Kast, Cytotoxic T lymphocytes raised against a subdominant epitope offered as a synthetic peptide eradicate human papillomavirus type 16-induced tumors. Eur J Immunol, 1995. 25(9): p. 2638-42.
18. van Montfoort, N., M.G. Camps, S. Khan, D.V. Filippov, J.J. Weterings, J.M. Griffith, H.J. Geuze, T. van Hall, J.S. Verbeek, C.J. Melief, and F. Ossendorp, Antigen storage compartments in mature dendritic cells facilitate prolonged cytotoxic T lymphocyte cross-priming capacity. Proc Natl Acad Sci U S A, 2009. 106(16): p. 6730-5.
19. Schuurhuis, D.H., A. Ioan-Facsinay, B. Nagelkerken, J.J. van Schip, C. Sedlik, C.J. Melief, J.S. Verbeek, and F. Ossendorp, Antigen-antibody immune complexes empower dendritic cells to efficiently prime specific $CD8^+$ CTL responses *in vivo*. J Immunol, 2002. 168(5): p. 2240-6.
20. Rogošiy, M., H.J. Mencer, and Z. Gomzi, Polydispersity index and molecular weight distributions of polymers. European Polymer Journal, 1996. 32(11): p. 1337–1344.
21. King, C.G., S. Koehli, B. Hausmann, M. Schmaler, D. Zehn, and E. Palmer, T cell affinity regulates asymmetric division, effector cell differentiation, and tissue pathology. Immunity, 2012. 37(4): p. 709-20.
22. Zehn, D., C. King, M.J. Bevan, and E. Palmer, TCR signaling requirements for activating T cells and for generating memory. Cell Mol Life Sci, 2012. 69(10): p. 1565-75.
23. Rudd, B.D., J.D. Brien, M.P. Davenport, and J. Nikolich-Zugich, Cutting edge: TLR ligands increase TCR triggering by slowing peptide-MHC class I decay rates. J Immunol, 2008. 181(8): p. 5199-203.
24. Chen, L. and M. Jondal, Alternative processing for MHC class I presentation

by immature and CpG-activated dendritic cells. Eur J Immunol, 2004. 34(4): p. 952-60.
25. Chen, L. and M. Jondal, Brefeldin A inhibits vesicular MHC class I processing in resting but not in CpG- and disruption-activated DC. Mol Immunol, 2008. 46(1): p. 158-65.
26. Chen, L. and M. Jondal, Endolysosomal processing of exogenous antigen into major histocompatibility complex class I-binding peptides. Scand J Immunol, 2004. 59(6): p. 545-52.
27. Rock, K.L., D.J. Farfan-Arribas, and L. Shen, Proteases in MHC class I presentation and cross-presentation. J Immunol, 2010. 184(1): p. 9-15.
28. Joffre, O.P., E. Segura, A. Savina, and S. Amigorena, Cross-presentation by dendritic cells. Nat Rev Immunol, 2012. 12(8): p. 557-69.
29. Compeer, E.B., T.W. Flinsenberg, S.G. van der Grein, and M. Boes, Antigen processing and remodeling of the endosomal pathway: requirements for antigen cross-presentation. Front Immunol, 2012. 3: p. 37.
30. Sijts, E.J. and P.M. Kloetzel, The role of the proteasome in the generation of MHC class I ligands and immune responses. Cell Mol Life Sci, 2011. 68(9): p. 1491-502.
31. Baltazar, G.C., S. Guha, W. Lu, J. Lim, K. Boesze-Battaglia, A.M. Laties, P. Tyagi, U.B. Kompella, and C.H. Mitchell, Acidic nanoparticles are trafficked to lysosomes and restore an acidic lysosomal pH and degradative function to compromised ARPE-19 cells. PLoS One, 2012. 7(12): p. e49635.
32. Horiguchi, M., M. Arita, D.E. Kaempf-Rotzoll, M. Tsujimoto, K. Inoue, and H. Arai, pH-dependent translocation of alpha-tocopherol transfer protein (alpha-TTP) between hepatic cytosol and late endosomes. Genes Cells, 2003. 8(10): p. 789-800.
33. Shen, H., A.L. Ackerman, V. Cody, A. Giodini, E.R. Hinson, P. Cresswell, R.L. Edelson, W.M. Saltzman, and D.J. Hanlon, Enhanced and prolonged cross-presentation following endosomal escape of exogenous antigens encapsulated in biodegradable nanoparticles. Immunology, 2006. 117(1): p. 78-88.
34. Demento, S.L., S.C. Eisenbarth, H.G. Foellmer, C. Platt, M.J. Caplan, W. Mark Saltzman, I. Mellman, M. Ledizet, E. Fikrig, R.A. Flavell, and T.M. Fahmy, Inflammasome-activating nanoparticles as modular systems for optimizing vaccine efficacy. Vaccine, 2009. 27(23): p. 3013-21.
35. Panyam, J., W.Z. Zhou, S. Prabha, S.K. Sahoo, and V. Labhasetwar, Rapid endo-lysosomal escape of poly(DL-lactide-co-glycolide) nanoparticles: implications for drug and gene delivery. FASEB J, 2002. 16(10): p. 1217-26.
36. Hamdy, S., O. Molavi, Z. Ma, A. Haddadi, A. Alshamsan, Z. Gobti, S. Elhasi, J. Samuel, and A. Lavasanifar, Co-delivery of cancer-associated antigen and Toll-like receptor 4 ligand in PLGA nanoparticles induces potent $CD8^+$ T cell-mediated anti-tumor immunity. Vaccine, 2008. 26(39): p. 5046-57.
37. Mueller, M., W. Reichardt, J. Koerner, and M. Groettrup, Coencapsulation of tumor lysate and CpG-ODN in PLGA-microspheres enables successful immunotherapy of prostate carcinoma in TRAMP mice. J Control Release, 2012. 162(1): p. 159-66.
38. Mueller, M., E. Schlosser, B. Gander, and M. Groettrup, Tumor eradication by immunotherapy with biodegradable PLGA microspheres--an alternative to

incomplete Freund's adjuvant. Int J Cancer, 2011. 129(2): p. 407-16.
39. Zhang, Z., S. Tongchusak, Y. Mizukami, Y.J. Kang, T. Ioji, M. Touma, B. Reinhold, D.B. Keskin, E.L. Reinherz, and T. Sasada, Induction of anti-tumor *cytotoxic T cell responses through PLGA-nanoparticle mediated antigen delivery.* Biomaterials, 2011. **32**(14): p. 3666-78.

6. Supplemental Figures

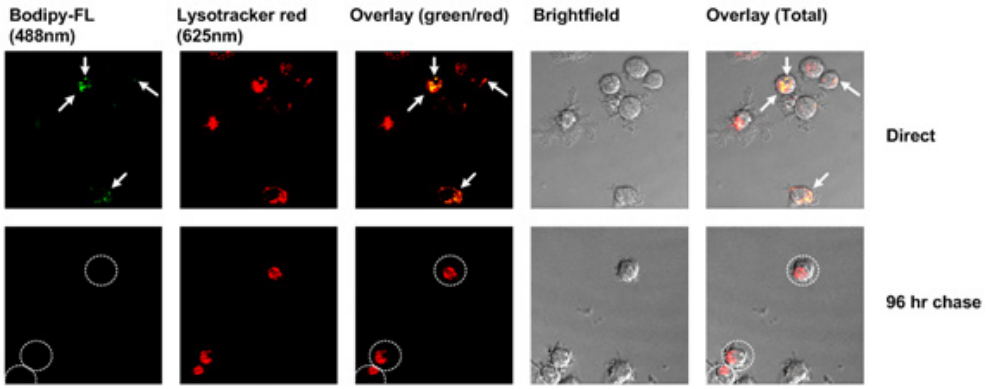

Supplemental Figure 1. Endosomal localisation of whole protein after internalization does not lead to prolonged Ag presence. D1 cells were incubated with 20 µM ovalbumin-Alexa488 (excitation- 488nm, visualized as the green signal) for 2.5 hr and either directly analyzed (upper panels) or further cultured in the absence of additional Ag or stimuli for 96 hr (lower panels). Co-staining with Lysotracker red was performed for visualization of the endo-lysosomes (red signal) and visualized by confocal microscopy. 1st column shows images depicting green signal as the fluorescence of the dye (488nm). 2nd column shows images depicting red signal as the fluoresence of the lysotracker red/endo-lysosomes (625nm). 3rd column depicts overlay images of red/green. Yellow-overlay signal marks co-localization. Images were analyzed using Leica software.

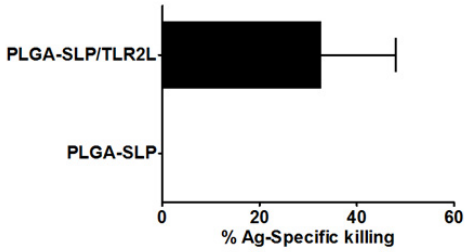

Supplemental Figure 2. Vaccinations with PLGA-SLP/TLR2L but not PLGA-SLP induces CD8⁺ T cells with *in vivo* cytotoxic capacity. Priming efficacy of endogenous cytotoxic CD8⁺ T cells by PLGA-SLP formulations, mice were vaccinated with 20 nmol SLP encapsulated in PLGA with or without Pam3CSK4 co-encapsulated. On day 7 post-vaccination, SIINFEKL-loaded (OVA-specific) target and control-target cells were injected. To obtain OVA-specific target cells, splenocytes from naïve congeneic C57BL/6 Ly5.1 mice were pulsed for 1 h with 1 µM of SIINFEKL-peptide and co-stained with 10 µM CFSE (CFSE-high) (Molecular Probes, Eugene, OR). As a negative control, 1 µM of the immunodominant ASNENMETM-peptide derived from the influenza virus nucleoprotein co-stained with 0.5 µM CFSE (CFSE-low) was used. Specific and non-specific target cells were mixed 1:1 and injected intravenously (i.v.; 10 x 106 cells of each population). 18 hr after cells were transferred, mice were sacrificed and spleen cells were harvested to prepare single cell suspensions that were then subjected to flow cytometric analysis. Injected cells were distinguished by APC-conjugated rat anti-mouse CD45.1 mAb. The percentage specific killing was calculated as follow: 100 - ([(% SIINFEKL-peptide pulsed in treated/% ASNENMETM-pulsed in treated)/(% SIINFEKL-peptide pulsed in non-treated/% ASNENMETM-pulsed in non-treated)] x 100).